Molecular Microbiology (2001) **42**(4), 967–979

Structure of the type III secretion and substrate-binding domain of *Yersinia* YopH phosphatase

Craig L. Smith,[1,2†] Purnima Khandelwal,[2] Kai Keliikuli,[2] Erik R. P. Zuiderweg[1,2,3] and Mark A. Saper[1,2*]
[1]*Department of Biological Chemistry,* [2]*Biophysics Research Division and* [3]*Department of Chemistry, University of Michigan, 930 N. University Ave., Ann Arbor, MI 48109-1055, USA.*

Summary

Pathogenic strains of *Yersinia* deploy a type III secretion system to inject the potent tyrosine phosphatase YopH into host cells, where it dephosphorylates focal adhesion-associated substrates. The amino-terminal, non-catalytic domain of YopH is bifunctional; it is essential for the secretion and binding of the specific chaperone SycH, but also targets the catalytic domain to substrates in the infected cell. We describe the 2.2 Å resolution crystal structure of residues 1–129 of YopH from *Yersinia pseudotuberculosis*. The amino-terminal α-helix (2–17), comprising the secretion signal, and β-strand (24–28) of one molecule exchange with another molecule to form a domain-swapped dimer. Nuclear magnetic resonance (NMR) and gel filtration experiments demonstrated that YopH(1–129) could exist as a monomer and/or a dimer in solution. The topology of the dimer and the dynamics of a monomeric form in solution observed by NMR imply that YopH has the propensity to unfold partially. The dimer is probably not important physiologically, but may mimic how SycH binds to the exposed non-polar surfaces of a partially unfolded YopH. Phosphopeptide-induced perturbations in NMR chemical shifts define a substrate-binding surface on YopH(1–129) that includes residues previously shown by mutagenesis to be essential for YopH function.

Introduction

Bacterial pathogens use unique ways to control their animal and plant hosts. A primary strategy is to modulate the signal transduction pathways of the host. Many Gram-negative bacteria, including species of *Escherichia*, *Salmonella*, *Yersinia*, *Xanthomonas* and *Erwinia*, do this by translocating effector proteins (virulence factors) directly into the host cell cytoplasm (Finlay and Cossart, 1997; Hueck, 1998; Cornelis and Van Gijsegem, 2000). Delivery is by a contact-dependent type III secretion system, termed an injectosome or secreton, which spans both bacterial and animal cell membranes. A similar type III system is found in the basal body of bacterial flagella (Macnab, 1999).

Three *Yersinia* species – *Yersinia pestis*, the aetiological agent of plague, and *Yersinia pseudotuberculosis* and *Yersinia enterocolitica* that cause gastrointestinal disorders – encode the injectosome on a 70 kb plasmid that is absolutely required for virulence. *Yersinia* translocates six effectors into host macrophages (Hueck, 1998). One of them, YopH (468 residues), is a modular protein consisting of a non-catalytic region (residues 1–130) and a potent tyrosine phosphatase domain (residues 190–468), which is very similar to eukaryotic enzymes in both structure and catalytic mechanism (Guan and Dixon, 1990; Zhang and Dixon, 1994; Fauman and Saper, 1996). YopH was shown to be essential for virulence in mice (Bliska *et al.*, 1991). By dephosphorylating cytoskeletal proteins in infected macrophages, it effectively disrupts phosphotyrosine-dependent signalling pathways necessary for phagocytosis (Bliska *et al.*, 1992; Andersson *et al.*, 1996). Host protein targets include Crk-associated substrate ($p130^{Cas}$), paxillin and focal adhesion kinase in HeLa cells (Black and Bliska, 1997; Persson *et al.*, 1997), and Cas/Fyn-binding protein and murine SKAP-HOM in macrophages (Hamid *et al.*, 1999; Black *et al.*, 2000).

Removal of the amino-terminal domain of YopH prevents the secretion and translocation of YopH by the type III system. Using various truncation mutations fused to a reporter gene, residues 1–17 were identified as necessary and sufficient for secretion, whereas residues 18–71 were necessary for translocation into the infected cell (Sory *et al.*, 1995). Unlike type II secreted proteins, the YopH amino-terminal domain does not share a conserved signal sequence with other type III secreted proteins, nor is it cleaved by a signal peptidase. This suggests that the type III injectosome may recognize a structural motif or chemical property that is an integral part of the effector protein's overall structure. Lloyd *et al.* (2001) have suggested that an amphipathic helix may be the recognition motif. Furthermore, YopH, like many other

Accepted 11 September, 2001. *For correspondence at the Biophysics Research Division. E-mail saper@umich.edu; Tel. (+1) 734 764 3353; Fax (+1) 734 764 3323. †Present address: Department of Molecular Microbiology, Washington University School of Medicine, St Louis, MO 63110, USA.

© 2001 Blackwell Science Ltd

Table 1. Diffraction data and refinement statistics[a].

Crystal	Native	K_2PtCl_4 (10 mM, 24 h)	UO_2Cl_2 (10 mM, 24 h)	$HgCl_2$ (1 mM, 24 h)
Resolution (Å)	22.0–2.2 (2.28–2.20)	22.0–2.1 (2.18–2.10)	22.0–2.2 (2.26–2.20)	22.0–2.7 (2.80–2.70)
λ (Å)	1.5418	1.07142[b]	1.5418	1.5418
Total measurements[c]	68 285 (NA[d])	98 870 (NA)	98 744 (NA)	24 038 (NA)
Unique reflections[e]	7503 (720)	8520 (785)	7486 (561)	3965 (379)
Redundancy[e]	6.2 (6.1)	6.3 (4.9)	6.7 (6.5)	2.6 (2.7)
Completeness (%)	99.8 (99.9)	98.7 (93.8)	97.2 (73.8)	96.1 (99.2)
$<I/\sigma_I>$	20.8 (16.2)	15.7 (7.2)	23.6 (17.6)	12.9 (5.7)
R_{sym}	0.050 (0.136)	0.066 (0.223)	0.053 (0.142)	0.081 (0.221)
MIRAS phasing				
Resolution (Å)	20–2.2 (2.48–2.20)	20–2.2 (2.48–2.20)	20–2.2 (2.48–2.20)	20–2.5 (2.83–2.48)
Number of sites		2	2	2
Phasing power		1.44 (1.30)	0.98 (0.87)	1.15 (1.19)
R_{cullis}		0.95 (1.07)	0.91 (1.02)	0.85 (0.92)
% reflections with anomalous differences[f]		83.2 (86.4)	85.4 (88.8)	–
$<\lvert F_{PH}(+)-F_{PH}(-)\rvert>/<F_{PH}>$[f]		0.041 (0.075)	0.047 (0.076)	
Anomalous R_{cullis}[f]		0.94 (1.01)	0.92 (0.99)	–
Figure of merit	0.46 (0.28)			
After density modification	0.66 (NA)			
Refinement statistics				
Resolution (Å)	22.0–2.2 (2.25–2.20)			
Number of reflections				
Working set	6732 (461)			
Test set	747 (49)			
R_{work}	0.224 (0.222)			
R_{free}	0.258 (0.276)			
Number of atoms				
Total	1055			
Protein	945			
Solvent	110			
r.m.s.d. bond lengths (Å)	0.054			
r.m.s.d. bond angles (°)	1.115			
$<B>$ (Å^2)				
All	30.8			
Main chain	27.6			
Side-chain	32.3			
Solvent	39.6			

a. Phasing power and *R*-factors are defined in Drenth (1999). Values in parentheses are for the highest resolution shell.
b. K_2PtCl_4 derivative data collected at CHESS; this is the absorption peak wavelength. Other data collected on the R-AXIS IV.
c. Bijvoet-related measurements counted separately.
d. NA, value not available.
e. Bijvoet-related reflections/measurements counted as one reflection.
f. A low-resolution cut-off of 10 Å was applied to the anomalous data.

© 2001 Blackwell Science Ltd, *Molecular Microbiology*, **42**, 967–979

type III secreted effectors, must bind a specific chaperone protein for successful translocation. SycH, one of a family of acidic type III chaperone proteins, requires residues 20–70 of YopH for interaction (Woestyn *et al.*, 1996). In *Yersinia* mutants lacking SycH, YopH accumulates in the bacterial cytoplasm.

The YopH non-catalytic domain is multifunctional. Black *et al.* (1998) showed that, once inside the infected cell, the amino-terminal domain of YopH binds to phosphorylated proteins that are *in vivo* substrates of the phosphatase domain. This interaction is phosphotyrosine dependent and is important for efficient targeting of YopH to substrate. Subsequently, several residues implicated in this interaction were detected by random mutagenesis (Montagna *et al.*, 2001).

To understand how YopH is recognized for type III secretion and translocation, we describe the crystal structure of residues 1–129 of the YopH effector from *Y. pseudotuberculosis*. Unexpectedly, the molecule forms a domain-swapped dimer that may mimic an intracellular YopH:SycH complex. Additionally, we have mapped a phosphopeptide binding site on the protein with nuclear magnetic resonance (NMR) chemical shift perturbation data. We compare the results with a recently reported structure from a seemingly identical crystal form (Evdokimov *et al.*, 2001).

Results

YopH(1–129) forms a domain-swapped dimer

The structure of the amino-terminal, non-catalytic domain (residues 1–129) of YopH from *Y. pseudotuberculosis* was determined by multiple isomorphous replacement with anomalous scattering. YopH(1–129) is 100% and 98% identical to its homologues in *Y. pestis* and *Y. enterocolitica* respectively. The model, consisting of residues 2–125 and 110 water molecules, was refined to 2.2 Å resolution with an *R*-factor of 0.224 and $R_{free} = 0.258$. The crystallographic results are summarized in Table 1.

YopH(1–129) forms a domain-swapped dimer with a crystallographic dyad-related molecule (Bennett *et al.*, 1995) (Fig. 1). Overall dimensions of the dimer are about 54 Å × 37 Å × 40 Å. Each monomer adopts an $\alpha + \beta$ structure containing four α-helices and four β-strands (Fig. 1B). Residues 2–28, which form the α1-helix and the first half of the β1-strand, extend away from the rest of the monomer and interact primarily with the other subunit of the dimer. Following β1, residues 34–49 form an ordered meander that lacks apparent secondary structure except for a β-turn between residues 43 and 46. Following this are two antiparallel helices, α2 and α3, separated by a short β-strand (β2). Helix α3 is followed by a β-hairpin composed of strands β3 and β4. Together with β2, these form a three-stranded antiparallel sheet that forms a small platform for the three helices of the core domain. Following β4 is the α4-helix running parallel to α2 and antiparallel to α3. The final resolved residue in the structure is Ser-125. Residues 126–129 and the Ser-$(His)_6$ tag are presumed to be disordered. Searches of known protein folds failed to recognize any other structures with similarity to YopH(1–129).

The polypeptide regions in YopH suggested to be essential for type III secretion and translocation (Sory *et al.*, 1995) are highlighted in Fig. 1B. The secretion segment (residues 2–17) is simply the α1-helix, whereas the translocation domain (18–71) is made up of the β1-strand, the meandering loop, α2 and β2. The meandering loop (residues 35–49) connects the β1-strand to α2 and is part of the region shown to be essential for binding the specific chaperone SycH (Woestyn *et al.*, 1996). Its fold is maintained by an extensive hydrogen-bonding network (Fig. 2) primarily involving four residues: Thr-24 (from the other subunit), Asn-34, Glu-52 and Gln-107. Side-chains from each of these residues make hydrogen bonds to main-chain atoms of the loop. Within the loop, there is a prominent β-turn (43–46) that exposes an Ala and an Ile to solvent. A major conformational restraint of the loop is a salt bridge between Glu-36 and Arg-49 that 'pins' the loop together (Fig. 2).

In the dimer observed in the crystal structure, the β1-strand (24–34) pairs with β1 of the symmetry-related molecule to form an antiparallel twisted β-ladder with 8–10 interstrand hydrogen bonds. The 'swapped' α1-helix (2–17) packs against α2 and α4 of the other subunit, primarily through non-polar contacts. The total solvent-accessible surface of each subunit buried by dimer formation is ≈ 2540 Å^2 representing $\approx 30\%$ of the subunit surface area (Fig. 3). Approximately two-thirds of this surface is hydrophobic. The only other intersubunit contacts are between β1 and α2 and the two amino-termini.

YopH(1–129) exists as a monomer and dimer in solution

The result that YopH(1–129) crystallized as a domain-swapped dimer was unexpected. Previous studies demonstrated that full-length YopH was a monomer in solution (Zhang *et al.*, 1992). Although the full-length YopH had an apparent molecular weight of 74 000 based on size exclusion chromatography, sedimentation equilibrium showed a molecular weight of $\approx 49\,000$, suggesting an extended monomer in solution (Zhang *et al.*, 1992).

For crystallization, YopH(1–129) ($M_r \approx 14\,800$) was prepared in imidazole buffer at pH 7.2 and crystallized at pH 8 (see *Experimental procedures*). To investigate whether pH affected the oligomeric structure of YopH(1–129), cells expressing the same expression construct were lysed and purified at pH 5.7 with a procedure similar to that described for the full-length and catalytic domain forms of YopH (Zhang *et al.*, 1992). Gel filtration of both samples on

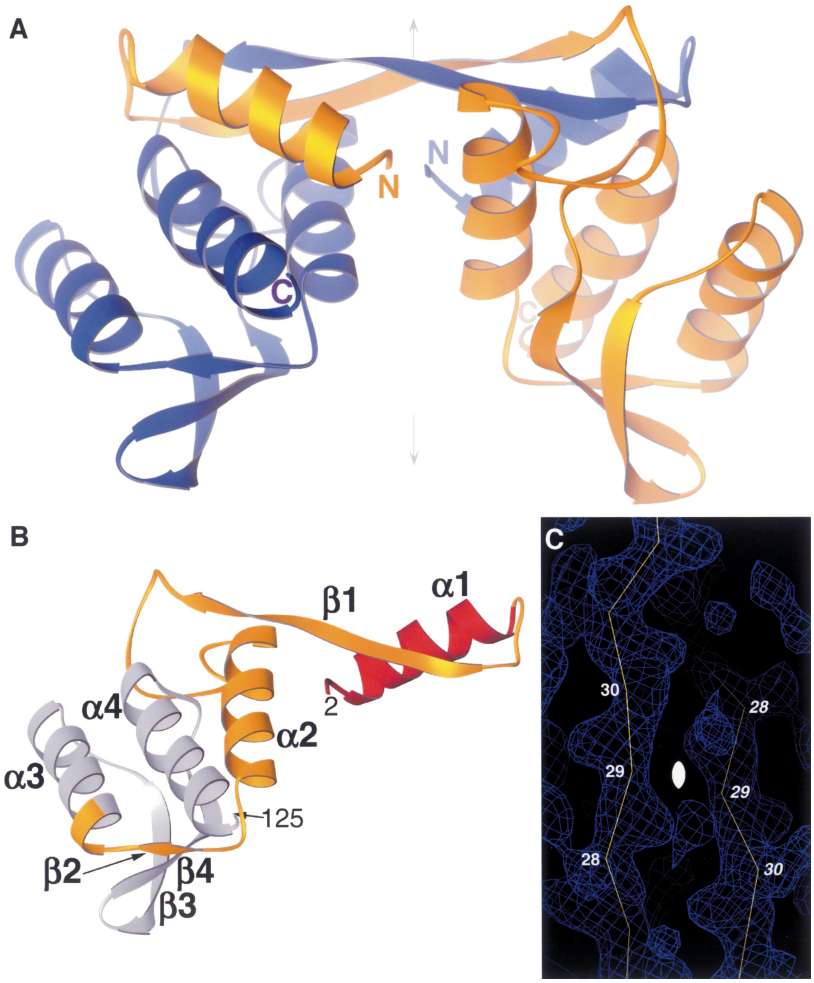

Fig. 1. Tertiary fold of YopH(1–129).
A. Domain-swapped dimer observed in the crystal structure. A crystallographic dyad (shown by arrow) relates the two molecules that comprise the dimer.
B. Structure of one subunit with regions shown previously to be important for secretion (red, residues 2–17), translocation (gold, residues 17–71) and chaperone binding (20–70) (Sory *et al.*, 1995; Woestyn *et al.*, 1996). The secondary structural elements are labelled. The N- and C-termini are residues 2 and 125 respectively.
C. Omit electron density map ($2F_{obs}-F_{calc}$, α_{calc}) contoured at 1σ in the region around the twofold axis relating the two subunits of the dimer. Gly-29 is the 'hinge' residue (Bennett *et al.*, 1995). In a monomeric structure, the polypeptide would probably form a reverse turn at this position (compare with Fig. 7A).

a calibrated Superdex 75 HR 10/30 column showed that the protein purified at pH 7.2 contained two species with apparent molecular weights of 29 800 (major peak) and 15 300, whereas the low pH preparation was predominantly one species with an apparent molecular weight of 13 300 (Fig. 4A). The poor separation of the pH 7.2 species may reflect a dynamic equilibrium between monomer and dimer. Nevertheless, further purification of each species can be achieved, and the two forms are stable at low pH (J. Vijayalakshmi, data not shown). Dynamic light scattering

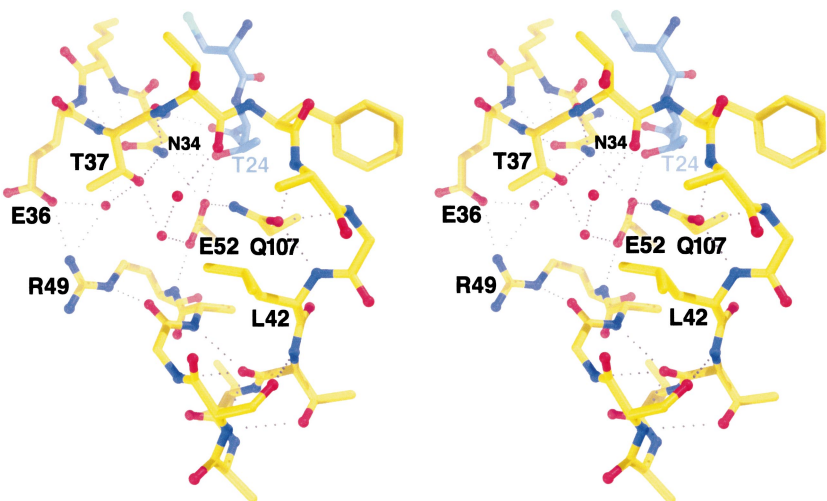

Fig. 2. Stereo pair of the meandering loop (35–49) fold. Atoms are coloured by type: C, yellow; N, blue; O, red; S, cyan. Light blue carbon atoms are from the symmetry-related subunit. Hydrogen bonds are dashed lines, and red spheres are ordered water molecules. Loop includes residues involved in peptide binding and comprises part of the region shown to be important for binding the SycH chaperone.

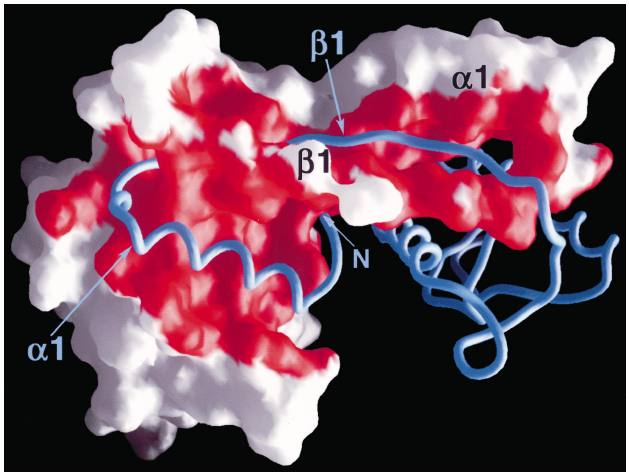

Fig. 3. Contact surface between subunits in the YopH(1–129) dimer. Molecular surface of one subunit showing contacts less than 4 Å (red surface) with the other subunit (depicted by the blue tube). Prepared in GRASP (Nicholls *et al.*, 1991).

measurements (data not shown) of the pH 7.2 protein showed a monodisperse species with hydrodynamic radius of 2.7 nm, consistent with an apparent molecular weight of 32 000. Protein prepared at pH 5.7 had a radius of 2.1 nm, which would correspond to a globular protein of about 17 kDa (also see below). Interestingly, isoelectric focusing (data not shown) of the protein purified at pH 7.2 showed five bands with pI values ranging from 7.4 to 8.0 (theoretical pI = 8.03), whereas the protein at pH 5.7 was a single isoform of pI = 8.0. These experiments suggest that, when overexpressed in *Escherichia coli*, YopH(1–129) folds into both monomers and dimers, but the monomeric form appears to predominate at low pH. Recent results have demonstrated that purified dimer was stable at all pH values tested, but that the purified monomer slowly aggregated when shifted to higher pH (J. Vijayalakshmi, unpublished data).

Because of the ability of YopH(1–129) to form both monomeric and dimeric forms, we wished to assess whether the protein in solution had any conformational flexibility. NMR spin relaxation methods use the $^{15}N-^{1}HN$ bond vector as a probe to sense protein backbone dynamics (Peng and Wagner, 1994). Nitrogen-15 R_2 relaxation rates were measured for ^{15}N-labelled YopH(1–129) at pH 6.5 in phosphate buffer (Fig. 4B). The average T_2 relaxation time ($1/R_2$) for the majority of residues was 90 ms. The mean value for the T_1 ($1/R_1$) was 876 ms (results not shown). From these values, we calculated a rotational correlation time of 7.1 ns, which corresponds to

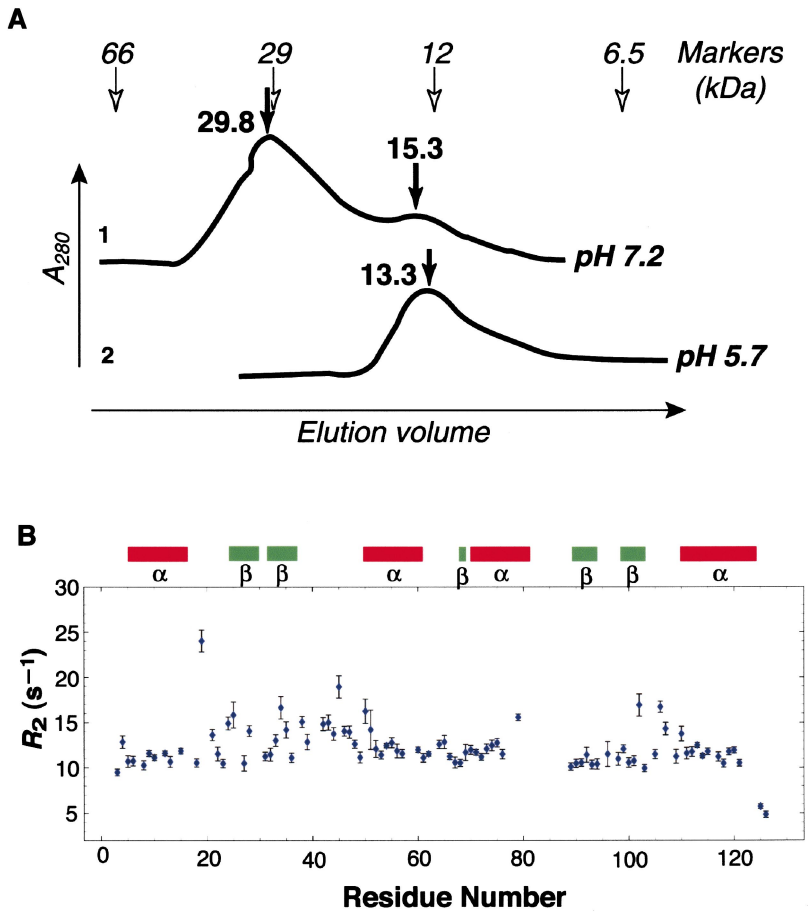

Fig. 4. Solution studies of YopH(1–129).
A. YopH(1–129) samples were injected into a Superdex 75 HR 10/30 column connected to a Waters liquid chromatography system. Trace 1 is protein purified at pH 7.4 by the Ni^{2+}-NTA column, dialysed in imidazole buffer, pH 7.2, and eluted in the same buffer. The broadness of the two peaks could mean that interconversion between monomeric and dimeric forms may be taking place during the experiment. Trace 2 is the protein purified at pH 5.7 and eluted with 100 mM NaCl, 1 mM EDTA, 100 mM sodium acetate, pH 5.7. Peak locations of molecular weight standards (Sigma) are shown above the traces and were used to interpolate the YopH(1–129) protein peak molecular weights.
B. ^{15}N T_2 relaxation in YopH(1–129). R_2 values ($1/T_2$) are plotted as a function of residue number. Error bars reflect experimental errors in measurement. Missing data points result from residues that did not have assigned resonances. Secondary structures assigned from the crystal structure are shown. Regions showing higher than average R_2 values reflect conformational averaging and are located mostly in the loops.

a hydrodynamic radius of 1.99 nm, using the Stokes–Einstein relationship (Cavanagh *et al.*, 1996). This number is in excellent agreement with the hydrodynamic radius of 2.1 nm obtained from the dynamic light scattering studies at low pH described above and a theoretical value of 1.94 nm predicted for a 14.8 kDa protein, assuming a single hydration shell and a specific volume of $0.73\,cm^3\,g^{-1}$ (Cavanagh *et al.*, 1996). This proves that YopH(1–129) is a monomer of 14.8 kDa in solution at pH 6.5 or lower, even at the relatively high concentration of 0.9 mM used for the NMR studies.

By examining the R_2 values for individual residues (Fig. 4B), we noted that certain residues, mainly located between helices α1 and α2 (residues 19–50), showed considerably greater line broadening of their ^{15}N resonances (up to $15\,s^{-1}$ excess broadening). This indicates that these regions in the monomeric protein are undergoing conformational exchange (i.e. adopting different conformations) at the milli- to microsecond timescale. This conformationally dynamic portion of the monomer corresponds to the domain cross-over region (β1 and the meandering loop) in the dimer (see Fig. 1B). In contrast, these residues appear to be static in the dimer observed in the crystal structure, as they have average crystallographic temperature factors that are even slightly below those of the entire dimer ($<B> = 25.7\,Å^2$ for residues 20–50 compared with $<B> = 29.2\,Å^2$ for all residues).

YopH(1–129) binds tyrosine-phosphorylated peptides

In addition to its role in secretion, translocation and chaperone binding by *Yersinia*, the amino-terminal domain of YopH also binds to proteins in the infected host cell known to be substrates for the YopH phosphatase domain (Black *et al.*, 1998). Binding is phosphotyrosine dependent with specificity similar to that of the Crk SH2 domain. YopH(1–129) lacks significant sequence or tertiary structure similarity to other targeting domains such as the SH2 and PTB domains. The former are present on the amino-termini of several eukaryotic tyrosine phosphatases (Hof *et al.*, 1998).

Recently, Montagna *et al.* (2001) identified four residues (Gln-11, Val-31, Ala-33 and Asn-34) in the amino-terminal domain of YopH that were important for binding to phosphorylated $p130^{cas}$, an *in vivo* substrate of YopH. Residues 31–34 are on the part of β1 that packs against the α1-helix coming from the other subunit, and Gln-11 is nearby on the exposed surface of α1 (magenta side-chains in Fig. 5D). Val-31, Ala-33 and Gln-11 surround a

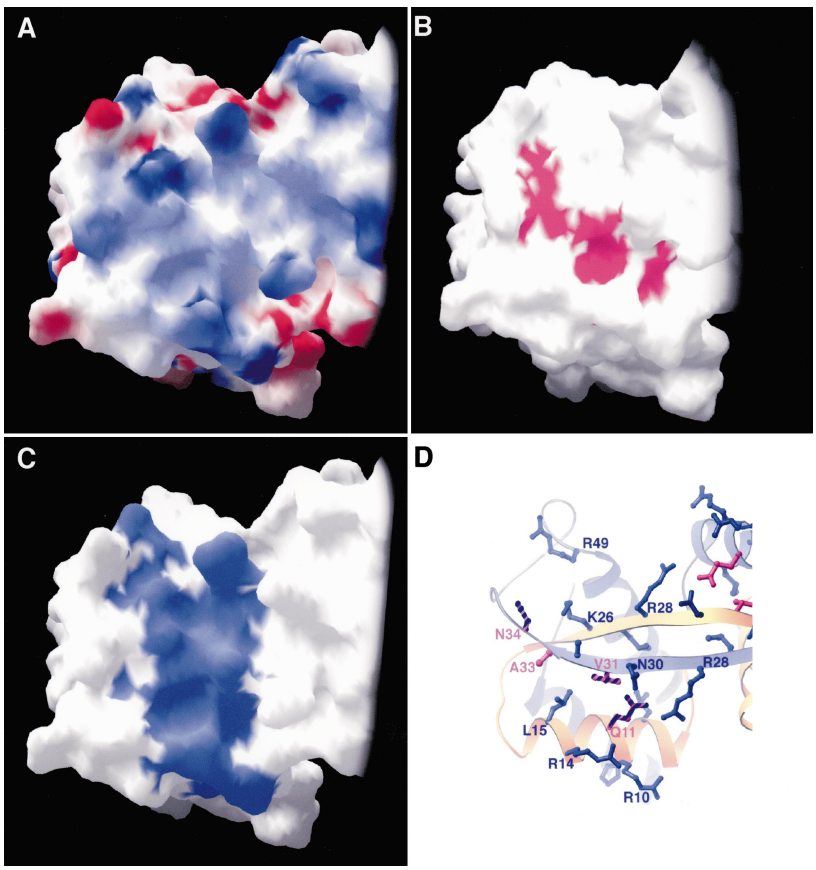

Fig. 5. Phosphopeptide-binding region on YopH(1–129). Molecule is rotated ≈ 90° along the horizontal from Fig. 1A. Only the left half of the dimer is shown.
A. The solvent contact surface is coloured by electrostatic potential (red is negative; blue is positive).
B. The magenta coloured surface indicates the four residues (Gln-11, Val-31, Ala-33 and Asn-34) that, when mutated, interfered with binding to phosphorylated $p130^{Cas}$ (Montagna *et al.*, 2001).
C. Highlighted in blue are residues of YopH(1–129) that have perturbed chemical shifts when YopH(1–129) was titrated with the phosphopeptide acetyl-DE(pY)DDPF-NH2.
D. Ribbon representation of this portion of YopH(1–129) showing the location of side-chains implicated in forming the phosphopeptide-binding region. Side-chain colours are as in (B) and (C). Residues 11, 31 and 34 were identified by both NMR and mutagenesis.

pronounced pocket formed between α1 and β1 (Fig. 5B and D). The Gln-11 side-chain also anchors the α1-helix to the β1-strand through two hydrogen bonds. Although this is an intersubunit interaction, it would also exist in a monomeric structure (see *Discussion*). Asn-34 is only partially solvent accessible, but constrains the conformation of the meandering loop by hydrogen bonding to Thr-37 and Glu-52 (see Fig. 2).

To assess those residues actually involved in phosphopeptide binding, doubly labelled [^{15}N, ^{13}C]-YopH(1–129) was titrated with a concentrated solution of the phosphopeptide acetyl-DE(pY)DDPF-amide derived from murine SKAP-HOM, a YopH substrate (Black *et al.*, 2000). The binding process for this peptide is in the slow/intermediate exchange regime, indicating on- and off-rates of the order of milliseconds or slower. Residues 8–11, 14–15, 26–28, 30–32, 34 and 49 had chemical shifts that were significantly different compared with the apoprotein (Khandelwal *et al.*, 2001) (Fig. 5C and D). Atoms from these perturbed residues are probably located in the vicinity of a bound phosphopeptide or have undergone conformational changes to shift their chemical environment. These residues, of which three were also identified by mutagenesis, form a wide, mostly electropositive patch over the surface of α1 and the two β1-strands (Fig. 5A and D). Notably, six of these 14 residues are positively charged, appropriate for binding such an acidic peptide. Residues Arg-14, Leu-15 and Asn-30 surround the pocket containing Val-31, Ala-33 and Gln-11 mentioned above. Next to this pocket is a positive depression with Arg-28, Arg-14 and Arg-10, all of which undergo changes upon peptide binding.

YopH(1–129) and LcrQ are structurally similar proteins

Searching sequence databases (NCBI, September 2000) with PSI-BLAST failed to detect any other sequence similar to YopH(1–129) except for two proteins previously reported to have significant sequence homology: LcrQ (termed YscM1 in *Y. enterocolitica*) and YscM2 (only in *Y. enterocolitica*) (Rimpiläinen *et al.*, 1992; Stainier *et al.*, 1997). Surprisingly, these are also found on the *Yersinia* virulon. LcrQ and YscM2 are 33% and 29% identical, respectively, to YopH(1–129) (Fig. 6). *Yersinia* strains containing *lcrQ* deletions secreted Yop effectors constitutively at 37°C independent of Ca^{2+} concentration. It was hypothesized that LcrQ may act as a negative repressor of *yop* gene transcription (Rimpiläinen *et al.*, 1992). Recently, it was reported that SycH, the chaperone specific for YopH, also binds to LcrQ and is necessary for its translocation (Cambronne *et al.*, 2000). The carboxy-terminal regions of all three proteins are more homologous than the amino-terminus (Fig. 6), suggesting that most of LcrQ could fold like YopH. Hydrophobic residues in helix α1 (positions 5, 8, 12 and 16) are conserved in all three proteins. This suggests that the amphipathic nature of this helix element may be a determinant for type III secretion.

There are two deletions in LcrQ and YscM2. One is a seven-residue deletion (22–28) in the β1-strand. This may suggest that these proteins cannot form dimers like YopH. This region also contains two of the five positively charged residues (Lys-26 and Arg-28) implicated in substrate binding by YopH(1–129). The second deletion (residues 79–83) is at the end of helix α3 and includes Lys-82, which forms a salt bridge to Asp-22. None of the surface residues involved in the proposed YopH(1–129) substrate binding site are conserved in the other two proteins, pointing to the unique role of YopH for binding host cell substrates.

Discussion

The dimer may mimic the YopH:SycH interaction

In the crystal structure described here, the amino-terminal domain of YopH, residues 1–129, forms a domain-swapped dimer in which residues 2–28 from one protein molecule associate almost exclusively with another molecule related by a crystallographic dyad (180°

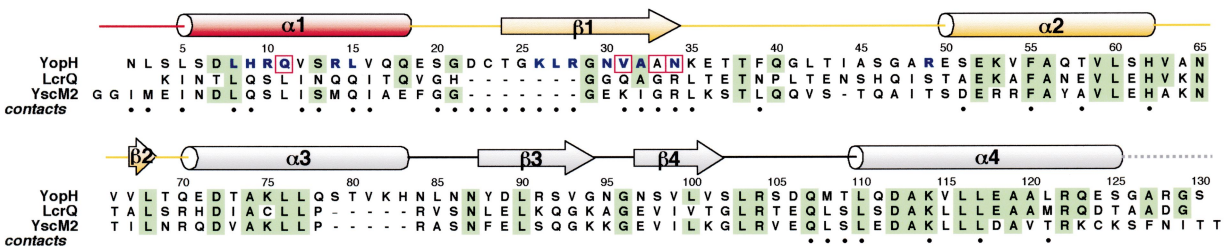

Fig. 6. Sequence alignment of YopH(1–129) with two homologous proteins. The sequences are YopH (*Y. pseudotuberculosis*), LcrQ (*Y. pseudotuberculosis*; 33% identical) and YscM2 (*Y. enterocolitica*; 29% identical). YopH residues are coloured green if they are identical to LcrQ and/or YscM2. The *Y. pestis* LcrQ gene is 100% identical to *Y. pseudotuberculosis* LcrQ, whereas *Y. enterocolitica* YscM1 is 99% identical. Secondary structure designations of YopH(1–129) are displayed above the sequence alignment using the same colour scheme as in Fig. 1B. Alpha-helices are depicted as cylinders and β-strands as arrows. Residues in blue had perturbed chemical shifts upon binding phosphopeptide. Residues boxed in magenta are those that, when mutated, inhibited p130^{Cas} binding (Montagna *et al.*, 2001). Residues with a black dot make intersubunit contacts in the YopH(1–129) dimer. Residue numbering is for YopH.

rotation). Domain swaps have been observed in numerous other proteins; recent examples include RNase A (Liu *et al*., 2001), SH2 domain (Schiering *et al*., 2000) and Hsp-33 (Vijayalakshmi *et al*., 2001). In some cases, three-dimensional domain swapping can occur at high protein concentration or through changes in pH, temperature or buffer composition (Bennett *et al*., 1995). But there are cases in which the dimer is physiologically important (Newcomer, 2001) or implies biological function (e.g. Su *et al*., 1998). Most probably, the YopH(1–129) dimer has no physiological role in secretion, but the mode of interaction suggests how the specific chaperone SycH may bind to YopH.

The results presented here show that the recombinant protein as purified can adopt a monomeric conformation in solution and that it is the major species when the protein is purified at pH 5.7. The NMR relaxation measurements in phosphate buffer at pH 6.5 described here and a forthcoming NMR structure determination of a phosphopeptide complex (P. Khandelwal *et al*., in preparation) are consistent with a monomeric form. The fold of the monomeric form is identical to half the observed dimer (as in Fig. 7A, see next page) and preserves most of the intramolecular interactions observed in the dimer. Instead of the main chain of the 10-residue β1-strand forming hydrogen bonds to β1 of the other subunit in the dimer, the monomeric structure has a tight turn at Gly-29 with β1 folding back on itself to form a two-stranded β-hairpin.

A dimeric form of YopH(1–129) also exists in solution, as shown by the dynamic light scattering and gel filtration analyses. The dimer in the crystal is topologically intertwined (knotted); simply translating the two monomers away from each other cannot separate the two subunits. Considering the topology, the monomeric form of YopH(1–129) must partially unfold before forming a dimer. Such a scenario would require α1 to dissociate from the core domain, the turn between α1 and β1 to open and the meandering loop (33–49) between β1 and α2 to unravel partially. In fact, the NMR relaxation data show that extensive conformational exchange processes at the milli- to microsecond timescale do occur in this region of the monomeric form (residues 20–50), part of which is the dimer cross-over strand (residues 23–31). It is conceivable that this region of the monomer adopts various conformations in solution, including a partially unfolded form, which could serve as an intermediate on the dimer-folding pathway. We suspect that YopH as well as the amino-terminal regions of other type III secreted proteins are partially unfolded and/or flexible, and that this conformation may be essential for biological function (reviewed by Namba, 2001). Such conformations can associate with other proteins, either specifically or non-specifically, and may include chaperones, transcription factors or components of the injectosome. For example, FlgM, an antisigma factor secreted by the flagellar type III system, has a disordered amino-terminus when studied by solution NMR that becomes ordered upon binding to RNA polymerase (Daughdrill *et al*., 1997; 1998).

With the previous points in mind, we suggest that the YopH(1–129) dimer observed in the crystal might be mimicking the interactions in the complex formed between the amino-terminal region of YopH and its specific chaperone SycH. SycH may immediately bind the exposed hydrophobic regions on a nascent YopH polypeptide or in a single, partially unfolded monomer. These regions in the partially unfolded monomer include residues 5, 8, 12, 15 and 16 from α1, 25, 27, 31, 32 and 33 from β1, 54, 55 and 59 from α2 and 110, 113, 117 and 121 from α4. The β1 and α2 regions are part of the polypeptide segment shown previously to be essential for chaperone binding (Woestyn *et al*., 1996). By binding to these surfaces, SycH prevents YopH from aggregating with itself or other proteins, a phenomenon that was observed in a *sycH*$^-$ mutant strain of *Yersinia* (Woestyn *et al*., 1996). By binding to an extended YopH(1–129), SycH may present the α1-helix (containing the previously implicated secretion signal 1–17) for docking on the ATPase (YscN in *Yersinia*) and subsequent threading through the injectosome. This may promote further unfolding downstream during membrane translocation. Note that the α1-helix and its similar counterpart in LcrQ are amphipathic, a property previously suggested in YopE to be the primary recognition element for secretion (Lloyd *et al*., 2001).

SycH may also bind to the apparently flexible meandering loop (35–49) and restrain its conformation. The alignment in Fig. 6 indicates that this loop is also present in LcrQ. Confirming the structural role of SycH and its mode of binding to YopH or LcrQ must await structural characterization of a complex.

Comparison with another YopH(1–129) structure determination

During the preparation of this report, a crystal structure was reported of a very similar construct of YopH(1–129) (PDB entry 1HUF; Evdokimov *et al*., 2001). The crystal space group, unit cell parameters, position of the molecule in the unit cell and the overall structure of 1HUF are very similar to that reported here. The only difference between 1HUF and the structure presented here is that the 1HUF polypeptide was modelled as a compact monomer, with a reverse γ-turn centred on Gly-29 to form a β-hairpin (β1 and β2 in the 1HUF nomenclature). Otherwise, the two crystal structures are identical (Fig. 7).

From these considerations, we propose that the electron density in both crystal structures is most consistent with a domain-swapped dimer rather than with a compact monomer. The protein purified by Evdokimov *et al*.

(2001) was crystallized with a pH 9 precipitant, which is close to the pH 8.5 precipitant used in the present work. From our observations, high pH and protein concentration promote protein dimerization (J. Vijayalakshmi, unpublished). Difference electron density maps were calculated for the 1HUF structure using the deposited structure factors in the Protein Data Bank (PDB entry r1hufsf) and for the structure and data described in this report. In both cases, residues 27–31 had been omitted and the model refined by simulated annealing. Comparison of the location of difference peaks showed them to be very similar (data not shown). There was no positive electron density above 2σ for Gly-29 in a γ-turn conformation in either structure. Moreover, atoms from the 1HUF tight turn make several close and improbable intermolecular contacts with those of the identical turn in the symmetry-related molecule (e.g. the symmetry-related Gly-29 α-carbons are 2.5 Å apart; asterisk in Fig. 7A). This symmetry-related molecule in the present structure corresponds to a subunit of the domain-swapped dimer (Fig. 7B).

The phosphopeptide-binding surface

We have described solution NMR experiments that show direct binding of a phosphopeptide to the amino-terminal domain of YopH. This allowed mapping the residues perturbed by binding, and these overlap three residues previously identified by mutagenesis (Montagna *et al.*, 2001). Although the substrate-binding domain has no structural homology to an SH2 domain, it appears to be serving a similar role. The Crk-associated protein p130^{cas} previously identified as a YopH substrate (Black and Bliska, 1997) contains ≈ 15 Tyr-containing motifs (YxxP) typical of the recognition sequence for the SH2 domain of

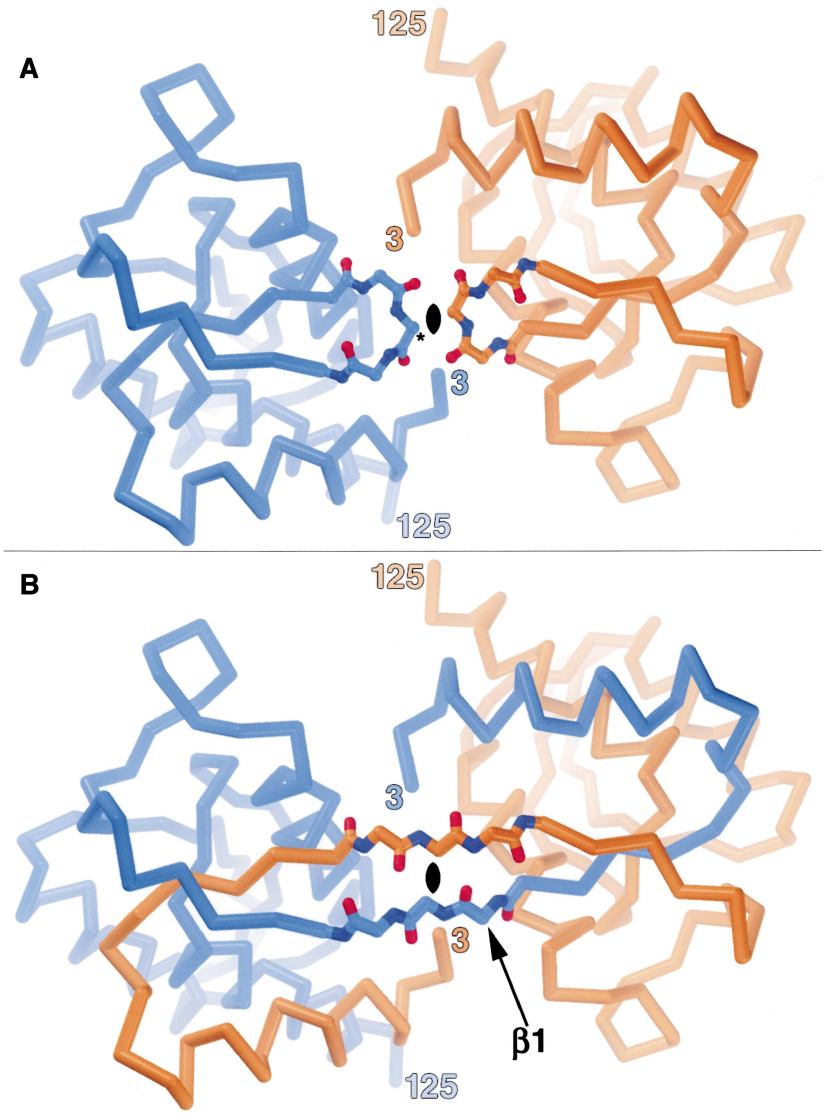

Fig. 7. Comparison of similar YopH(1–129) crystal structures. The view in both images is perpendicular to the crystallographic dyad parallel to the *b*-axis (black symbol) and located at $x+\frac{1}{2}$, $z+\frac{1}{4}$; in each of the unit cells. The orientation and position of the molecule in the unit cells are identical in (A) and (B). Without superposition, the r.m.s.d. between main-chain atoms is 0.37 Å for residues 3–27 and 31–125.
A. The 1HUF structure (Evdokimov *et al.*, 2001) modelled as a monomer (left) and its dyad-related symmetry molecule (right). The asterisk indicates the Gly-29 Cα of the β-turn that is 2.5 Å from its symmetry mate.
B. The swapped dimer structure (this work) with β1-strands crossing between subunits.

Crk (Birge *et al.*, 1993; Sakai *et al.*, 1994). The phosphopeptide used in the NMR experiments is from another YopH substrate that also contains this motif (Black *et al.*, 2000). It is envisaged that the amino-terminal domain of YopH will bind to one of the phosphorylated motifs and increase the apparent affinity or specificity of the catalytic domain towards the phosphotyrosine of a nearby motif (Black *et al.*, 1998).

We have provided evidence that the phosphopeptide-binding region is composed of residues from the α1-helix, the β1-hairpin of a proposed monomer and Arg-49 from the end of the meandering loop. The highly positive charged surface is suitable for recognizing the substrates of YopH that contain not only the negatively charged phosphotyrosine but also other acidic residues nearby. The NMR data do not show any global changes in line width during the titration, so the possibility that the protein unfolds to bind substrate is unlikely. It may, in fact, stabilize the structure. Exactly how the phosphopeptide is positioned with respect to this surface must await the NMR structure of the peptide–protein complex (P. Khandelwal *et al.*, in preparation).

Experimental procedures

Purification and crystallization

Expression plasmid pYopH (Bliska and Black, 1995), modified to encode residues 1–129 of *Y. pseudotuberculosis* YopH fused to a Ser-$(His)_6$ tag, was provided by Professor James B. Bliska (State University of New York, Stony Brook, NY, USA). Transformed *E. coli* BL21(DE3) cells were grown in LB media, induced with 1 mM IPTG for 2 h at 37°C and harvested by centrifugation. Frozen cell pellets were resuspended in lysis buffer containing 137 mM NaCl, 3 mM KCl, 10 mM Na_2HPO_4, 2 mM KH_2PO_4, pH 7.4, and protease inhibitors: aprotinin (0.05 μg ml^{-1}), leupeptin (0.05 μg ml^{-1}) and tosyl-L-lysine chloromethyl ketone (0.5 mg ml^{-1}). Cells were lysed by two passes through a French press (1200 p.s.i.) and clarified by centrifugation at 20 400 *g* for 20 min. The supernatant was mixed with 5 ml of Ni^{2+}-NTA matrix (Qiagen) equilibrated in lysis buffer and rocked gently for 1 h at 4°C. After washing the gel three times with lysis buffer and three times with lysis buffer containing 30 mM imidazole, the protein was eluted with a linear gradient from 30 to 300 mM imidazole. The protein was > 99% pure by SDS–gel electrophoresis. Before crystallization, the protein was dialysed into 10 mM NaCl, 1 mM EDTA, 0.1% β-mercaptoethanol, 10 mM imidazole, pH 7.2, and concentrated to 10 mg ml^{-1} in a Centricon 10 (Millipore) at 4°C. Drops containing 2 μl of protein and 2 μl of precipitant [2–10% polyethylene glycol (PEG) 8000, 90–100 mM NaCl, 100 mM Tris-HCl, pH 8.5] were equilibrated against 1 ml of the same precipitant by vapour diffusion at 22°C. Triangular crystals appeared in 24 h and grew to full size ($0.45 \times 0.4 \times 0.2$ mm^3) in 3–5 days. Crystals were of space group $C222_1$ with cell dimensions $a = 47.9$ Å, $b = 120.7$ Å, $c = 48.8$ Å and one molecule per asymmetric unit.

For NMR studies, [^{15}N, ^{13}C]-YopH(1–129) was prepared by growing bacteria in M9 minimal media supplemented with [^{13}C]-glucose and $^{15}NH_4Cl$. A ^{15}N-labelled sample was prepared using $^{15}NH_4Cl$. Protein was purified as above, dialysed into sample buffer (5% ^2H_2O, 0.05% NaN_3, 50 mM sodium phosphate, pH 6.5) and concentrated to 0.8–0.9 mM.

Data collection

Before data collection, crystals in stabilizing solution (10% PEG 8000, 90 mM NaCl, 100 mM Tris-HCl, pH 8.6) were transferred to the same solution containing 20% 2-methyl, 2,4-pentanediol for 3–5 min and frozen with cold nitrogen gas generated by the X-stream system (Molecular Structure). $HgCl_2$ and UO_2Cl_2 derivative and native intensity data were measured with an R-AXIS IV (Rigaku) detector using X-rays generated by an RU-3-HR running at 50 kV, 100 mA and double focusing mirrors (Molecular Structure). Platinum chloride derivative data were collected at the L_{III} edge of platinum using the Princeton CCD detector at beamline F2, Cornell High Energy Synchrotron Source. Images were processed with the HKL package (Otwinowski and Minor, 1997) and the CCP4 system (Bailey, 1994).

Phasing and refinement

Heavy atom sites for the platinum derivative were located in isomorphous and anomalous difference Patterson maps. Binding sites for the other derivatives ($HgCl_2$ and UO_2Cl_2) were determined by difference Fourier methods. The heavy atom positions were refined and the MIRAS phases calculated with MLPHARE (Bailey, 1994). Solvent flattening and histogram matching with DM improved the phases. The initial chain trace into 3.0 Å solvent-flattened maps located all secondary structural elements. Successive rounds of model building with the program O (Jones *et al.*, 1991), refinement of the partial structure with X-PLOR and phase combination using SIGMAA (Read, 1986) allowed for an unambiguous tracing of the protein from residues 2–125. Omit maps helped to clarify the domain swap at the crystallographic twofold (Fig. 1C). The model, including a bulk solvent term and 110 water molecules, was refined to 2.2 Å resolution with good stereochemistry. Residues 126–136, which include the $(His)_6$ tag, were not visible in the electron density and believed to be disordered. Refinement statistics are presented in Table 1. Co-ordinates and structure factors have been deposited in the Protein Data Bank (http://www.rcsb.org; accession code 1K46). Figures were prepared with RIBBONS (Carson, 1997), O (Jones *et al.*, 1991), MCMOLW and MCSHOWCASE (McRee, 1996) and GRASP (Nicholls *et al.*, 1991).

Purification of YopH(1–129) monomer

The monomeric form of YopH(1–129) was expressed from the same plasmid described above, but purified by a procedure similar to that reported for the full-length YopH (Zhang *et al.*, 1992). Cell pellets were suspended in 100 mM NaCl, 1 mM EDTA, 0.1% β-mercaptoethanol (v/v), 100 mM sodium acetate, pH 5.7. Cleared lysates were added to a CM-Sepharose cation exchange column. The column was washed twice with 300 mM NaCl in acetate buffer and eluted with a

linear 0.5–1.5 M NaCl gradient. Pure fractions were collected, concentrated and dialysed in 10 mM NaCl, 1 mM EDTA, 0.1% β-mercaptoethanol, 10 mM sodium acetate, pH 5.7. The protein was applied to a Superdex HR 75 10/30 gel filtration column (Amersham Pharmacia Biotech) and eluted with the same buffer. The apparent molecular weights of the eluted peaks were estimated by comparison with elution volumes of protein standards. Dynamic light scattering was done with the Dyna-Pro 801 (Protein Solutions). Apparent molecular weights were derived from the hydrodynamic radius using the manufacturer's software.

NMR T_1 and T_2 relaxation measurements

NMR spectra for ^{15}N spin relaxation measurements and peptide titrations were recorded on a Varian 800 MHz Inova spectrometer at 25°C, using a sample of ≈ 0.9 mM in sodium phosphate buffer, pH 6.5. ^{1}H, ^{15}N and ^{13}C chemical shifts were assigned to backbone and side-chain atoms as described previously (Khandelwal *et al*., 2001). T_1 relaxation times were measured according to established methods (Dayie and Wagner, 1994). The T_2 experiment was recorded as published (Dayie and Wagner, 1994), with the modification that only a single ^{15}N refocusing pulse and continuous proton decoupling were used in the T_2 measuring period (Wang *et al*., 2001). Without the CPMG or spin-lock sequence, conformational exchange broadening, signifying milli- and microsecond dynamics, was maximally preserved. All experiments were recorded as 128*4096 complex matrices with 16 scans per complex t_1 point and spectral width of 3000 Hz and 15009 Hz in the F1 and F2 dimensions with recycle delay of 1 s. For T_1 measurements, 15 inversion recovery delays varying from 10 to 1100 ms were used. Fourteen transverse relaxation delays from 10 to 100 ms were used for T_2 measurements. Duplicate experiments were recorded for a few delays. The spectra were processed and analysed using NMRPIPE (Delaglio *et al*., 1995) and NMRVIEW (Johnson and Blevins, 1994) respectively. The relaxation rates were obtained from non-linear fits of single exponential functions for longitudinal and transverse relaxation.

Peptide titration using HSQC experiments

To assess phosphopeptide binding to YopH(1–129), two-dimensional ^{1}H–^{15}N HSQC spectra were collected at increasing concentrations of the peptide acetyl-DE(pY)DDPF-amide (synthesized at the University of Michigan Protein Structure Facility). Aliquots of a 12 mM peptide solution in water were added to 840 μl of 0.9 mM protein solution to give peptide–protein molar ratios of 0.07, 0.15, 0.30, 0.45, 0.61, 0.76, 0.91, 1.06 and 1.2. The ^{15}N–^{1}H HSQC spectra were overlaid, and peaks that changed their chemical shifts in a continuous fashion (fast/intermediate exchange) were identified. In addition, resonances for the peptide complex were assigned independently of the apoprotein (Khandelwal *et al*., 2001), which allowed the identification of the titrating residues in intermediate/slow exchange. Residues were defined as perturbed upon peptide binding if the chemical shift of two nuclei had changed significantly between complex and apoprotein.

Acknowledgements

We are grateful to Dr James Bliska for stimulating this research. We also thank J. Vijayalakshmi for sharing unpublished results, and past and present members of the Saper and Ludwig laboratories. Funding was provided by NIH grants to M.A.S and E.R.P.Z. Peptide syntheses at the University of Michigan Biomedical Research Core Facilities were subsidized by the U-M Comprehensive Cancer and Multipurpose Arthritis Centers. We thank the scientists at CHESS and its support from the NIH and DOE.

References

Andersson, K., Carballeira, N., Magnusson, K.E., Persson, C., Stendahl, O., Wolf-Watz, H., and Fallman, M. (1996) YopH of *Yersinia pseudotuberculosis* interrupts early phosphotyrosine signalling associated with phagocytosis. *Mol Microbiol* **20**: 1057–1069.

Bailey, S. (1994) The CCP4 suite of programs for protein crystallography. *Acta Crystallogr D Biol Crystallogr* **50**: 760–763.

Bennett, M.J., Schlunegger, M.P., and Eisenberg, D. (1995) 3D domain swapping: a mechanism for oligomer assembly. *Protein Sci* **4**: 2455–2468.

Birge, R.B., Fajardo, J.E., Reichman, C., Shoelson, S.E., Songyang, Z., Cantley, L.C., and Hanafusa, H. (1993) Identification and characterization of a high-affinity interaction between v-Crk and tyrosine-phosphorylated paxillin in CT10-transformed fibroblasts. *Mol Cell Biol* **13**: 4648–4656.

Black, D.S., and Bliska, J.B. (1997) Identification of p130^{Cas} as a substrate of *Yersinia* YopH (Yop51), a bacterial protein tyrosine phosphatase that translocates into mammalian cells and targets focal adhesions. *EMBO J* **16**: 2730–2744.

Black, D.S., Montagna, L.G., Zitsmann, S., and Bliska, J.B. (1998) Identification of an amino-terminal substrate-binding domain in the *Yersinia* tyrosine phosphatase that is required for efficient recognition of focal adhesion targets. *Mol Microbiol* **29**: 1263–1274.

Black, D.S., Marie-Cardine, A., Schraven, B., and Bliska, J.B. (2000) The *Yersinia* tyrosine phosphatase YopH targets a novel adhesion-regulated signalling complex in macrophages. *Cell Microbiol* **2**: 401–414.

Bliska, J.B., and Black, D.S. (1995) Inhibition of the Fc receptor-mediated oxidative burst in macrophages by the *Yersinia pseudotuberculosis* tyrosine phosphatase. *Infect Immun* **63**: 681–685.

Bliska, J.B., Guan, K.L., Dixon, J.E., and Falkow, S. (1991) Tyrosine phosphate hydrolysis of host proteins by an essential *Yersinia* virulence determinant. *Proc Natl Acad Sci USA* **88**: 1187–1191.

Bliska, J.B., Clemens, J.C., Dixon, J.E., and Falkow, S. (1992) The *Yersinia* tyrosine phosphatase: specificity of a bacterial virulence determinant for phosphoproteins in the J774A.1 macrophage. *J Exp Med* **176**: 1625–1630.

Cambronne, E.D., Cheng, L.W., and Schneewind, O. (2000) LcrQ/YscM1, regulators of the *Yersinia yop* virulon, are injected into host cells by a chaperone-dependent mechanism. *Mol Microbiol* **37**: 263–273.

Carson, M. (1997) Ribbons. *Methods Enzymol* **277**: 493–505.

Cavanagh, J., Fairbrother, W.J., Palmer, A.G., III, and Skelton, N.J. (1996) *Protein NMR Spectroscopy: Principles and Practice*. San Diego: Academic Press.

Cornelis, G.R., and Van Gijsegem, F. (2000) Assembly and function of type III secretory systems. *Annu Rev Microbiol* **54**: 735–774.

Daughdrill, G.W., Chadsey, M.S., Karlinsey, J.E., Hughes, K.T., and Dahlquist, F.W. (1997) The C-terminal half of the anti-sigma factor, FlgM, becomes structured when bound to its target, sigma 28. *Nature Struct Biol* **4**: 285–291.

Daughdrill, G.W., Hanely, L.J., and Dahlquist, F.W. (1998) The C-terminal half of the anti-sigma factor FlgM contains a dynamic equilibrium solution structure favoring helical conformations. *Biochemistry* **37**: 1076–1082.

Dayie, K.T., and Wagner, G. (1994) Relaxation-rate measurements for ^{15}N-^{1}H groups with pulsed-field gradients and preservation of coherence pathways. *J Magn Reson A* **111**: 121–126.

Delaglio, F., Grzesiek, S., Vuister, G.W., Zhu, G., Pfeifer, J., and Bax, A. (1995) NMRPipe: a multidimensional spectral processing system based on UNIX pipes. *J Biomol NMR* **6**: 277–293.

Drenth, J. (1999) *Principles of Protein X-Ray Crystallography*. New York: Springer.

Evdokimov, A.G., Tropea, J.E., Routzahn, K.M., Copeland, T.D., and Waugh, D.S. (2001) Structure of the N-terminal domain of *Yersinia pestis* YopH at 2.0 Å resolution. *Acta Crystallogr D Biol Crystallogr* **57**: 793–799.

Fauman, E.B., and Saper, M.A. (1996) Structure and function of the protein tyrosine phosphatases. *Trends Biochem Sci* **21**: 413–417.

Finlay, B.B., and Cossart, P. (1997) Exploitation of mammalian host cell functions by bacterial pathogens. *Science* **276**: 718–725.

Guan, K.L., and Dixon, J.E. (1990) Protein tyrosine phosphatase activity of an essential virulence determinant in *Yersinia*. *Science* **249**: 553–556.

Hamid, N., Gustavsson, A., Andersson, K., McGee, K., Persson, C., Rudd, C.E., and Fallman, M. (1999) YopH dephosphorylates Cas and Fyn-binding protein in macrophages. *Microb Pathog* **27**: 231–242.

Hof, P., Pluskey, S., Dhe-Paganon, S., Eck, M.J., and Shoelson, S.E. (1998) Crystal structure of the tyrosine phosphatase SHP-2. *Cell* **92**: 441–450.

Hueck, C.J. (1998) Type III protein secretion systems in bacterial pathogens of animals and plants. *Microbiol Mol Biol Rev* **62**: 379–433.

Johnson, B.A., and Blevins, R.A. (1994) NMRView: a computer program for the visualization and analysis of NMR data. *J Biomol NMR* **4**: 603–614.

Jones, T.A., Zou, J.-Y., Cowan, S.W., and Kjeldgaard, M. (1991) Improved methods for building protein models in electron density maps and the location of errors in these models. *Acta Crystallogr A* **47**: 110–119.

Khandelwal, P., Keliikuli, K., Smith, C.L., Saper, M.A., and Zuiderweg, E.R.P. (2001) ^{1}H, ^{15}N and ^{13}C assignments of the N-terminal domain of *Yersinia* outer protein H in its apo form and in complex with a phosphotyrosine peptide. *J Biomol NMR* **21**: 69–70.

Liu, Y.S., Gotte, G., Libonati, M., and Eisenberg, D. (2001) A domain-swapped RNase A dimer with implications for amyloid formation. *Nature Struct Biol* **8**: 211–214.

Lloyd, S.A., Norman, M., Rosqvist, R., and Wolf-Watz, H. (2001) *Yersinia* YopE is targeted for type III secretion by N-terminal, not mRNA, signals. *Mol Microbiol* **39**: 520–531.

Macnab, R.M. (1999) The bacterial flagellum: reversible rotary propeller and type III export apparatus. *J Bacteriol* **181**: 7149–7153.

McRee, D. (1996) *Molecular Images Software* [http://www.concentric.net/~Molimage/]. San Diego: Molecular Images Software..

Montagna, L.G., Ivanov, M.I., and Bliska, J.B. (2001) Identification of residues in the N-terminal domain of the *Yersinia* tyrosine phosphatase that are critical for substrate recognition. *J Biol Chem* **276**: 5005–5011.

Namba, K. (2001) Roles of partly unfolded conformations in macromolecular self-assembly. *Genes Cells* **6**: 1–12.

Newcomer, M.E. (2001) Trading places. *Nature Struct Biol* **8**: 282–284.

Nicholls, A., Sharp, K.A., and Honig, B. (1991) Protein folding and association: insights from the interfacial and thermodynamic properties of hydrocarbons. *Proteins* **11**: 281–296.

Otwinowski, Z., and Minor, W. (1997) Processing of X-ray diffraction data collected in oscillation mode. *Methods Enzymol* **276**: 307–326.

Peng, J.W., and Wagner, G. (1994) Protein mobility from multiple ^{15}N relaxation parameters. In *Nuclear Magnetic Resonance Probes of Molecular Dynamics*. Tycko, R. (eds). Dordrecht: Kluwer, pp. 373–454.

Persson, C., Carballeira, N., Wolf-Watz, H., and Fallman, M. (1997) The PTPase YopH inhibits uptake of *Yersinia*, tyrosine phosphorylation of p130^{Cas} and FAK, and the associated accumulation of these proteins in peripheral focal adhesions. *EMBO J* **16**: 2307–2318.

Read, R.J. (1986) Improved Fourier coefficients for maps using phases from partial structures with errors. *Acta Crystallogr A* **42**: 140–149.

Rimpiläinen, M., Forsberg, Å., and Wolf-Watz, H. (1992) A novel protein, LcrQ, involved in the low-calcium response of *Yersinia pseudotuberculosis* shows extensive homology to YopH. *J Bacteriol* **174**: 3355–3363.

Sakai, R., Iwamatsu, A., Hirano, N., Ogawa, S., Tanaka, T., Mano, H., *et al.* (1994) A novel signaling molecule, p130, forms stable complexes *in vivo* with v-Crk and v-Src in a tyrosine phosphorylation-dependent manner. *EMBO J* **13**: 3748–3756.

Schiering, N., Casale, E., Caccia, P., Giordano, P., and Battistini, C. (2000) Dimer formation through domain swapping in the crystal structure of the Grb2–SH2–Ac-pYVNV complex. *Biochemistry* **39**: 13376–13382.

Sory, M.P., Boland, A., Lambermont, I., and Cornelis, G.R. (1995) Identification of the YopE and YopH domains required for secretion and internalization into the cytosol of macrophages, using the *cyaA* gene fusion approach. *Proc Natl Acad Sci USA* **92**: 11998–12002.

Stainier, I., Iriarte, M., and Cornelis, G.R. (1997) YscM1 and YscM2, two *Yersinia enterocolitica* proteins causing down-regulation of *yop* transcription. *Mol Microbiol* **26**: 833–843.

Su, X.D., Gastinel, L.N., Vaughn, D.E., Faye, I., Poon, P., and Bjorkman, P.J. (1998) Crystal structure of hemolin: a

horseshoe shape with implications for homophilic adhesion. *Science* **281**: 991–995.

Vijayalakshmi, J., Mukhergee, M.K., Graumann, J., Jakob, U., and Saper, M.A. (2001) The 2.2 Å crystal structure of Hsp33: a heat shock protein with redox-regulated chaperone activity. *Structure* **9**: 367–375.

Wang, L.C., Pang, Y.X., Holder, T., Brender, J.R., Kurochkin, A.V., and Zuiderweg, E.R.P. (2001) Functional dynamics in the active site of the ribonuclease binase. *Proc Natl Acad Sci USA* **98**: 7684–7689.

Woestyn, S., Sory, M.P., Boland, A., Lequenne, O., and Cornelis, G.R. (1996) The cytosolic SycE and SycH chaperones of *Yersinia* protect the region of YopE and YopH involved in translocation across eukaryotic cell membranes. *Mol Microbiol* **20**: 1261–1271.

Zhang, Z.-Y., and Dixon, J.E. (1994) Protein tyrosine phosphatases: mechanism of catalysis and substrate specificity. *Adv Enzymol Relat Areas Mol Biol* **68**: 1–36.

Zhang, Z.-Y., Clemens, J.C., Schubert, H.L., Stuckey, J.A., Fischer, M.W., Hume, D.M., *et al.* (1992) Expression, purification, and physicochemical characterization of a recombinant *Yersinia* protein tyrosine phosphatase. *J Biol Chem* **267**: 23759–23766.